



Published in final edited form as:

J Mol Cell Cardiol. 2015 October ; 87: 38–47. doi:10.1016/j.yjmcc.2015.07.032.

STIM1 elevation in the heart results in aberrant Ca^{2+} handling and cardiomyopathy

Robert N. Correll^{a,#}, Sanjeewa A. Goonasekera^{a,#}, Jop H. van Berlo^b, Adam R. Burr^a, Federica Accornero^a, Hongyu Zhang^c, Catherine A. Makarewich^c, Allen J. York^a, Michelle A. Sargent^a, Xiongwen Chen^c, Steven R. Houser^c, and Jeffery D. Molkentin^a

^aDepartment of Pediatrics, University of Cincinnati, Cincinnati Children's Hospital Medical Center, Howard Hughes Medical Institute, Cincinnati, Ohio, USA

^bDepartment of Medicine, Division of Cardiology, University of Minnesota, Minneapolis, Minnesota, USA

^cDepartment of Physiology, Temple University School of Medicine, Philadelphia, Pennsylvania, USA

Abstract

Stromal interaction molecule 1 (STIM1) is a Ca^{2+} sensor that partners with Orai1 to elicit Ca^{2+} entry in response to endoplasmic reticulum (ER) Ca^{2+} store depletion. While store-operated Ca^{2+} entry (SOCE) is important for maintaining ER Ca^{2+} homeostasis in non-excitabile cells, it is unclear what role it plays in the heart, although STIM1 is expressed in the heart and upregulated during disease. Here we analyzed transgenic mice with STIM1 overexpression in the heart to model the known increase of this protein in response to disease. As expected, STIM1 transgenic myocytes showed enhanced Ca^{2+} entry following store depletion and partial co-localization with the type 2 ryanodine receptor (RyR2) within the sarcoplasmic reticulum (SR), as well as enrichment around the sarcolemma. STIM1 transgenic mice exhibited sudden cardiac death as early as 6 weeks of age, while mice surviving past 12 weeks of age developed heart failure with hypertrophy, induction of the fetal gene program, histopathology and mitochondrial structural alterations, loss of ventricular functional performance and pulmonary edema. Younger, pre-symptomatic STIM1 transgenic mice exhibited enhanced pathology following pressure overload stimulation or neurohumoral agonist infusion, compared to controls. Mechanistically, cardiac myocytes isolated from STIM1 transgenic mice displayed spontaneous Ca^{2+} transients that were prevented by the SOCE blocker SKF-96365, increased L-type Ca^{2+} channel (LTCC) current, and enhanced Ca^{2+} spark frequency. Moreover, adult cardiac myocytes from STIM1 transgenic mice showed both increased diastolic Ca^{2+} and maximal transient amplitude but no increase in total SR

Corresponding author: Jeffery D. Molkentin, Cincinnati Children's Hospital Medical Center, Howard Hughes Medical Institute, Molecular Cardiovascular Biology, 240 Albert Sabin Way, MLC 7020, Cincinnati, Ohio 45229, USA. jeff.molkentin@cchmc.org.

[#]Authors contributed equally to this work.

Publisher's Disclaimer: This is a PDF file of an unedited manuscript that has been accepted for publication. As a service to our customers we are providing this early version of the manuscript. The manuscript will undergo copyediting, typesetting, and review of the resulting proof before it is published in its final citable form. Please note that during the production process errors may be discovered which could affect the content, and all legal disclaimers that apply to the journal pertain.

Disclosures

None.

Ca²⁺ load. Associated with this enhanced Ca²⁺ profile was an increase in cardiac nuclear factor of activated T-cells (NFAT) and Ca²⁺/calmodulin-dependent kinase II (CaMKII) activity. We conclude that STIM1 has an unexpected function in the heart where it alters communication between the sarcolemma and SR resulting in greater Ca²⁺ flux and a leaky SR compartment.

Keywords

calcium; hypertrophy; cardiac myocytes; heart failure; transgenesis

1. Introduction

Cardiac hypertrophy occurs as an adaptive response to increased hemodynamic load that initially preserves heart function, but eventually can lead to decompensation, heart failure and death. While remodeling associated with cardiac disease was first observed over 200 years ago [1], it is only in the past 25 years that the molecular pathways driving hypertrophic growth of the heart have begun to be delineated. Primary among them are Ca²⁺-responsive signaling pathways such as calcineurin/nuclear factor of activated T-cells (NFAT), protein kinase C and Ca²⁺/calmodulin-dependent protein kinase II (CaMKII) [2]. These effectors can be activated by Ca²⁺ flux through well-described Ca²⁺ entry pathways at the sarcolemma that include the cardiac L-type Ca²⁺ channel (LTCC) [3, 4], as well as nonspecific cation channels of the transient receptor potential (TRP) family [5–10], which are known mediators of store- and receptor-operated Ca²⁺ entry (SOCE and ROCE). While the role of SOCE in endoplasmic reticulum (ER) store repletion is well-appreciated in non-excitable cells, its importance is less clear in cardiac myocytes that exhibit rhythmic oscillations in intracellular Ca²⁺ [11] and contain robust mechanisms for Ca²⁺ loading of the sarcoplasmic reticulum (SR) via the sarcoplasmic/endoplasmic reticulum Ca²⁺ ATPase 2 (SERCA2) coupled with extracellular Ca²⁺ entry through the LTCC during each contractile cycle [12].

Despite the uncertain role for SOCE in normal cardiac myocyte physiology, recent studies have provided intriguing evidence that the Ca²⁺ sensor stromal interaction molecule 1 (STIM1) plays a role in cardiac Ca²⁺ regulation and disease. STIM1 is upregulated after pressure overload induced by transverse aortic constriction (TAC) [13], abdominal aortic banding [14] and phenylephrine (PE) infusion [13]. In addition, work from several groups has identified STIM1 as being required for hypertrophy in neonatal cardiac myocytes [13–15]. Additionally, knockdown of STIM1 in adult rats using an adeno-associated virus encoding a small hairpin RNA (shRNA) directed against STIM1 reduced cardiac hypertrophy, fibrosis and NFAT activation after pressure overload [14], supporting the notion that STIM1 participates in the development of cardiac hypertrophy in both neonatal myocytes and adult mice.

STIM1 is a membrane protein localized to the ER where it constitutively binds Ca²⁺ in the ER luminal space to sense its potential depletion. Reduction in ER Ca²⁺ results in loss of STIM1 Ca²⁺ binding leading to the clustering of this protein into multimeric complexes that then activate Orai1 in the plasma membrane to generate a Ca²⁺-selective channel that

reloads the ER directly from the extracellular space [16]. While STIM1 SOCE activity is due to its association with Orai1, recent work has shown interaction with a number of other Ca^{2+} regulatory proteins such as TRP channels [17], the LTCC [18, 19], SERCA2 [20, 21], the Na^+/K^+ ATPase [20], plasma membrane Ca^{2+} ATPase [20], and the type 1 ryanodine receptor (RyR1) [22, 23]. Relevant to its role in the repletion of ER Ca^{2+} stores, STIM1 activity may also activate Ca^{2+} and Na^+ influx through TRP channels in a manner similar to its effect on Orai1, resulting in a store-operated current [17], although this is still controversial [24].

Recently, our laboratory developed transgenic (TG) mice with restricted expression of STIM1 in both skeletal and cardiac muscle [22]. With respect to the heart, we observed that STIM1 overexpression results in enhanced refilling of intracellular Ca^{2+} following store depletion in isolated myocytes, as well as cardiac hypertrophy, activation of the fetal gene program, disrupted mitochondrial architecture, activation of Ca^{2+} -dependent NFAT and CaMKII pro-hypertrophic signaling pathways, enhanced SR Ca^{2+} cycling, and increased RyR2-dependent Ca^{2+} spark activity, ultimately leading to sudden death or heart failure.

2. Methods

STIM1 TG mice

TG mice with STIM1 overexpression in striated muscle were generated using the skeletal α -actin promoter [25], as described previously [22]. Three founder lines were generated and one line also showed expression of STIM1 in the heart, which was used in the current study. The NFAT-luciferase TG reporter mice were previously described [26]. All animal protocols were approved by the Institutional Animal Care and Use Committee at Cincinnati Children's Hospital Medical Center.

Western blot, mRNA analysis and electron microscopy

For western blot analysis, mice were sacrificed, hearts were surgically removed and snap frozen in liquid nitrogen and stored at -70°C . Ventricles were homogenized in modified RIPA buffer containing 50 mM Tris-HCl (pH 7.4), 150 mM NaCl, 0.25% sodium deoxycholate, 1 mM EDTA and protease inhibitors or a buffer containing 20 mM Tris-HCl (pH 7.5), 250 mM NaCl, 1% Triton X-100, 10 mM MgCl_2 , 0.5 mM dithiothreitol, and protease inhibitors. Homogenates were then centrifuged at 14,000 rpm for 10 minutes and the supernatants were used for blotting. Twenty-five to one hundred micrograms of protein were loaded on 6–15% SDS polyacrylamide gels suitable for detecting specific proteins relative to their molecular weights. Antibodies against STIM1 (Millipore), Orai1 (Millipore), TRPC1 (Santa Cruz), TRPC3 (Alomone), TRPC6 (Alomone), CaMKII δ (Abcam), phospho-RyR2 S2808 (Badrilla), phospho-RyR2 S2814 (Badrilla), total RyR (Santa Cruz), α -tubulin (Cell Signaling and Santa Cruz), NCX1 (Swant), SERCA2 (Badrilla), α -sarcomeric actin (Sigma), GAPDH (Fitzgerald Industries Intl.) and mitochondrial inner membrane proteins (MitoProfile total OXPHOS rodent western blot antibody cocktail, Abcam) were used. Detection was carried out via chemifluorescence with the Vistra ECF reagent (Amersham Pharmacia Biotech) and scanned with a Biorad Gel

Documentation center, or using fluorescent conjugated secondary antibodies (LI-COR) in combination with an Odyssey CLx Infrared Imaging System (LI-COR).

RNA was extracted from ventricles using the RNeasy Kit according to manufacturer's instructions (Qiagen). Reverse transcription was performed using the SuperScript III First-Strand Synthesis System (Invitrogen). Analysis of the hypertrophic markers was performed using individual Taqman gene expression assays (Applied Biosystems). Messenger RNA expression was quantified, normalized to RPL13 and expressed relative to control. Electron microscopy was performed on sections from wild-type (Wt) or STIM1 TG mice as previously described [27].

Isolation of adult cardiac myocytes and Ca^{2+} measurements

Adult mouse ventricular cardiac myocytes were isolated as previously described [8] in the presence of 10 mM 2,3-butanedione monoxime (BDM) or 25 μM blebbistatin. Cardiac myocytes were loaded with 2 μM Fura-2 acetoxymethyl ester (Invitrogen) for 15 min (or 35 min for SR load experiments) and placed in Tyrode's solution containing: 130 mM NaCl, 4 mM KCl, 2 mM CaCl_2 (or 0.5 mM CaCl_2 for SR load measurements), 1 mM MgCl_2 , 10 mM glucose, 10 mM HEPES (pH 7.4). The Fura-2 fluorescence ratio was determined using a delta scan dual-beam spectrofluorophotometer (Photon Technology International) or a dual-excitation fluorescence photomultiplier system (IonOptix) operated at an emission wavelength of 510 nm and excitation wavelengths of 340 and 380 nm. The stimulation frequency for Ca^{2+} transient measurements was 1 Hz. The stimulation frequency for SR load measurements was 0.5 Hz. Ca^{2+} traces were processed using a Savitzky-Golay filter and baseline Ca^{2+} levels, transient amplitude, and Ca^{2+} decay kinetics were analysed using Felix 1.1 and Ion Wizard (IonOptix) software.

For Ca^{2+} spark measurements, cardiac myocytes were loaded with 10 μM Fluo-4 (Invitrogen) for 15 min and then placed in Tyrode's solution containing: 140 mM NaCl, 4 mM KCl, 1.8 mM CaCl_2 , 1 mM MgCl_2 , 10 mM glucose, 5 mM HEPES (pH 7.4). Ca^{2+} sparks were recorded with a Nikon A1 confocal microscope using a GaAsP detector in line scan mode. The cells were stimulated at 0.5 Hz at least 15 times before stimulation was stopped and sparks were recorded at rest. The fluorophore was excited at 488 nm and emission maximum recorded at 525 nm. Sparks were counted using Sparkmaster [28] and ImageJ and calculated as sparks/100 $\mu\text{m/s}$.

Store operated Ca^{2+} entry was carried out as previously reported [22]. In brief, adult myocytes were loaded with 2 μM Fura-2 AM for 15 minutes then rinsed and incubated in Ca^{2+} and Mg^{2+} free (CMF) Ringer's solution with 30 μM cyclopiazonic acid (CPA) for 30 min. Myocytes were then rinsed with CMF/CPA solution and the Fura 2-AM excitation ratio (340/380 nm) was recorded. Measurements were made with a Nikon Eclipse Ti-U inverted microscope equipped with delta scan dual beam spectrofluorophotometer (Photon Technology, Birmingham, NJ). Following 2 minutes of CMF/CPA perfusion, the myocytes were perfused with 0.5 mM Ca^{2+} -containing Ringer's solution for a maximum of 5 minutes. Baseline to peak Ca^{2+} influx was taken as SOCE. For experiments in Figure 4, myocytes were incubated in CMF/CPA and perfused with 0 mM, 0.5 mM and 2 mM Ca^{2+} Ringer's solution for 3–5 minutes with or without 10 μM SKF-96365 (Tocris Bioscience).

Measurement of LTCC current using patch clamp methods

Patch clamp experiments were used to measure LTCC currents (I_{Ca-L}) in Wt and STIM1 TG myocytes. To isolate myocytes, after perfusion, the ventricles were separated from the atria, minced, and gently agitated in low Cl^- , high K^+ Kraft-Bruhe (KB) solution consisting of 50 mM glutamic acid, 40 mM KCl, 20 mM taurine, 20 mM KH_2PO_4 , 3 mM $MgCl_2$, 10 mM glucose, 1 mM EGTA, 10 mM HEPES pH 7.4. The dissociated cells were filtered through a nylon mesh and stored at 4°C in KB solution until use. Only Ca^{2+} -tolerant cells with clear cross-striations and without spontaneous contractions or significant granulation were selected for the experiments. All patch clamp experiments were conducted at room temperature (20–23°C) using a patch clamp amplifier (Axopatch200A; Axon Instruments). The recorded currents (I_{Ca-L}) were filtered at 2 kHz through a 4-pole low-pass Bessel filter and digitized at 5 kHz. The experiments were controlled using pClamp software (Axon Instruments) and analyzed using Clampfit. Current recordings were performed in bath solution superfused with the following Na^+ -free solution: 2 mM $CaCl_2$, 5 mM 4-aminopyridine, 136 mM tetraethylammonium-Cl (TEA-Cl), 1.1 mM $MgCl_2$, 25 mM HEPES, and 22 mM glucose (pH 7.4 with TEA-OH). The pipette solution contained: 100 mM cesium aspartate, 20 mM CsCl, 1 mM $MgCl_2$, 2 mM Mg-ATP, 0.5 mM Na_2 -GTP, 5 mM EGTA, 5 mM HEPES (pH 7.3 with 1N CsOH). I_{Ca-L} was measured by applying depolarizing voltage steps (380 ms)–40 mV to +60 mV, respectively, in 10-mV increments.

Echocardiography, pressure overload and drug treatment

Echocardiography was performed on isofluorane anesthetized mice using a Hewlett Packard 5500 instrument with a 15-MHz microprobe and measurements were taken on M-mode in triplicate for each mouse and averaged. Seven week-old mice of the relevant genotypes were subjected to a TAC or sham surgical procedure as previously described [26]. Doppler echocardiography was performed on mice subjected to TAC in order to determine pressure gradients across the aortic constriction. To generate additional models of cardiac disease, Alzet osmotic minipumps (no. 2002; Durect Corp) were dorsally implanted in anesthetized 7 week-old mice, for 2 weeks. The Alzet pumps were filled with solutions containing isoproterenol (60 mg/kg/d), or angiotensin II (432 μ g/kg/d) with phenylephrine (100 mg/kg/d), or phosphate buffered saline as a control for the experiments described in Figure 3.

CaMKII activity assay

CaMKII activity was determined using the SignaTect Ca^{2+} /calmodulin-dependent protein kinase assay system (Promega) according to the manufacturer's instructions. For the assay, homogenates were made from Wt or STIM1 TG hearts at 3.5 months of age using the following buffer: 10 mM Tris-HCl (pH 7.4), 150 mM NaCl, 1 mM dithiothreitol, 20% glycerol, 0.1% Triton X-100, 1× protease inhibitor cocktail (Calbiochem); protein concentration was determined by Bradford assay and CaMKII activity was determined from 2 μ g of protein.

Statistics

Results are presented in all cases as mean \pm SEM. Statistical analysis was performed using Prism 5 (Graphpad Software) or SigmaPlot for unpaired two-tailed t-tests. P-values less than 0.05 were considered significant.

3. Results

3.1 Overexpression of STIM1 results in enhanced Ca^{2+} influx

While the role of STIM1 in the heart is unclear, it is expressed at low levels and multiple laboratories have demonstrated upregulation of STIM1 during cardiac disease [13, 14]. To confirm these findings, we subjected Wt mice to pressure overload induced by 2 weeks of TAC surgery and showed induction of STIM1 protein via immunoblot (Figure 1A, and quantified in Figure 1B). Luo et al. have previously demonstrated that a longer isoform of STIM1 (STIM1L) is also induced in the heart after TAC [13]. Using an alternate antibody to STIM1 we also observed a higher molecular weight form of STIM1 only during pressure overload, but this appeared to be expressed at much lower levels than the lower molecular weight form of STIM1 (data not shown). To examine the potential effect of this increase in STIM1 expression in the diseased heart we utilized a mouse model with overexpression of STIM1 in the heart and skeletal muscle [22]. We confirmed that these mice show overexpression of STIM1 in the heart by western blotting (Figure 1C) that is at higher levels than observed during pressure overload stimulation. However, overexpression of STIM1 did not alter levels of associated SOCE proteins such as Orai1, TRPC1, TRPC3 or TRPC6 (Figure 1C). As expected, adult cardiac myocytes isolated from STIM1 TG mice showed a significant increase in Ca^{2+} influx using an *in vitro* store depletion assay, compared to myocytes isolated from wild-type (Wt) littermates (Figure 1D and quantified in Figure 1E). STIM1 overexpressed in our TG model displayed a peripheral pattern of localization that partially co-localized with RyR2 in regions adjacent to the surface sarcolemma (Figure 1F), a pattern distinct from that previously reported in adult mouse skeletal muscle, which showed complete co-localization of STIM1 with RyR1 through the entire myofiber [22, 23].

3.2 STIM1 overexpression causes sudden death and heart failure

Before 10 weeks of age STIM1 TG mice showed no significant changes in cardiac ventricular function as assessed by echocardiography, or differences in heart and lung weights compared to non-TG littermates (Figure 2A–C). However, by 14 weeks of age STIM1 TG mice began to show significantly decreased ventricular performance (Figure 2A), as well as increased heart weight and pulmonary edema (Figure 2B and C). The cardiac disease observed in STIM1 mice at 12 weeks of age was accompanied by re-activation of the fetal gene program including significantly increased expression of skeletal muscle α -actin (*Acta1*), β -myosin heavy chain (*Myh7*), atrial natriuretic factor (*Nppa*) and brain natriuretic peptide (*Nppb*) mRNA as determined by quantitative polymerase chain reaction (Figure 2E). In addition, STIM1 TG mice exhibited sporadic sudden death beginning at 6 weeks of age with complete lethality by 22 weeks of age (Figure 2D). Mice that perished before heart failure onset showed a typical profile of sudden death, which may be due to arrhythmia (see below).

Given that cardiac myocytes from STIM1 TG mice showed increased Ca^{2+} entry after store depletion, we hypothesized that mitochondrial function may be impaired due to Ca^{2+} overload in these hearts, similar to our previous observations in LTCC β_{2A} overexpressing TG mice [29]. Examination of cardiac histological sections via transmission electron microscopy revealed that STIM1 overexpressing hearts had swollen and degraded mitochondria with loosely-packed cristae, but western blot analysis showed no change in levels of the mitochondrial electron transport chain complexes (Figure 2F and G), similar to what was observed in the skeletal muscle of these TG mice [22].

3.3 STIM1 TG mice show enhanced disease with cardiac insult

We also investigated disease predisposition due to enhanced STIM1 expression by analyzing the mice before disease onset, in conjunction with known cardiac stress stimulation. STIM1 TG mice and Wt littermates were subjected to 2 weeks of pressure overload by TAC surgery at 7 weeks of age. STIM1 TG mice demonstrated significantly increased cardiac hypertrophy, reduced cardiac function and increased pulmonary edema (Figure 3A–C) suggesting induction of more fulminant heart disease compared to Wt controls. Because an increase in neurohumoral stimulation is closely associated with cardiac disease we also subjected a second cohort of 7 week-old STIM1 TG mice or Wt littermates to co-administration of angiotensin II with phenylephrine (AngII/PE) or isoproterenol for 2 weeks using Alzet osmotic minipumps. We similarly observed that STIM1 TG mice had significantly increased predisposition to cardiac hypertrophy and pulmonary edema, as well as increased fibrosis following AngII/PE infusion (Figure 3D–F, Supplemental Figure 1). Stimulation with isoproterenol had more subtle effects, but a significant increase in cardiac hypertrophy and pulmonary edema were observed in STIM1 TG mice compared with Wt littermates, with a trend towards reduced cardiac function (Figure 3G–I). These results collectively suggest that elevation of STIM1 levels in our TG mice predisposes the heart to enhanced disease after insult, further suggesting that increased STIM1 expression is a maladaptive alteration in the heart.

3.4 STIM1 overexpression results in spontaneous transients in isolated myocytes

Since cardiac myocytes isolated from STIM1 TG mice displayed increased Ca^{2+} entry following store depletion we investigated Ca^{2+} handling in more detail under standard conditions as described previously [8]. However, during the Ca^{2+} re-addition step we observed that the majority of STIM1 TG myocytes died compared to essentially none of the Wt controls (data not shown). Application of BDM or blebbistatin prevented this STIM1 TG myocyte death and allowed further experimentation, suggesting that increased Ca^{2+} entry and release was leading to overzealous myocyte contraction. However, adult cardiac myocytes from STIM1 TG mice still demonstrated spontaneous transients in a bath solution containing even low levels of Ca^{2+} , without electrical stimulation (Figure 4A). These transients were linked to extracellular Ca^{2+} and increased in amplitude in higher Ca^{2+} concentration solutions (Figure 4A). Additionally, these spontaneous transients were prevented by application of SKF-96365, an inhibitor of SOCE (Figure 4B), suggesting that STIM1-mediated enhancement of SOCE was responsible for initiating the increased Ca^{2+} cycling in the TG myocytes, in association with potentially much higher SR Ca^{2+} fluxing or leakage (see below).

3.5 STIM1 overexpression results in elevated Ca^{2+} cycling

We hypothesized that STIM1 overexpression resulted in augmented Ca^{2+} cycling in the heart. To determine if the activity of RyR2 was enhanced in association with greater SR Ca^{2+} cycling, we performed spark measurements on cardiac myocytes isolated from adult STIM1 TG mice or Wt littermate controls isolated with BDM, which was then removed after Ca^{2+} re-addition. As previously noted, STIM1 TG myocytes exhibited spontaneous transients and Ca^{2+} waves as shown in our representative line-scan images (Figure 5A, gray arrows). However, when quiescent regions between Ca^{2+} waves were analyzed and compared with those recorded from Wt myocytes shortly after stimulation, STIM1 TG myocytes demonstrated significantly higher spark frequencies, faster reuptake and reduced spark amplitude (Figure 5B–D). To extend these studies, we analyzed the spontaneous transients from a subset of cardiac myocytes isolated from STIM1 TG mice with spontaneous transients occurring at approximately 1 Hz and compared them to Wt control cardiac myocytes under 1 Hz field electrical stimulation in 2 mM Ca^{2+} bath solution. The results showed that STIM1 TG myocytes exhibited both significantly higher baseline (diastolic) Ca^{2+} levels and increased transient amplitude with more rapid Ca^{2+} decay kinetics compared with Wt control myocytes (Figure 6A–D). However, total SR Ca^{2+} load was not different between TG and Wt myocytes (Figure 6E). For this SR load experiment, STIM1 TG cardiac myocytes in 0.5 mM Ca^{2+} bath solution (to reduce spontaneous transient frequency and so avoid superposition of the caffeine transient) with spontaneous transients occurring at approximately 0.5 Hz were acutely treated with caffeine and the amplitude of the caffeine transient was compared to Wt control myocytes stimulated at 0.5 Hz and similarly treated with caffeine. Analysis of STIM1 TG spontaneous transients compared to Wt stimulated transients in 0.5 mM Ca^{2+} showed a similar increase in baseline Ca^{2+} levels and transient amplitude as were observed under 2 mM Ca^{2+} (data not shown). Overall these data suggest that elevated STIM1 results in enhancement of both Ca^{2+} uptake into the SR and RyR2-dependent Ca^{2+} efflux or leak, such that total SR Ca^{2+} load remains constant, in effect driving augmented Ca^{2+} cycling in transgenic myocytes.

Given that STIM1 has been reported to reduce LTCC activity and membrane occupancy [18, 19] independent of its roles in activation of SOCE, we also measured LTCC current activity using patch-clamp electrophysiology. Surprisingly, we observed that at 2 months of age, LTCC currents from STIM1 TG myocytes were augmented to the same level as Wt currents in the presence of the β -adrenergic agonist isoproterenol. Application of isoproterenol had no further effect on LTCC current from STIM1 TG myocytes, suggesting maximal channel activity (Figure 7A). This effect is likely short-lived, however, as immunoblotting for the $\alpha_1\text{c}$ pore forming subunit of the LTCC at a later time point (12 weeks of age) showed a decrease in expression, likely in compensation for the increased Ca^{2+} influx effect (Figure 7B).

3.6 STIM1-mediated Ca^{2+} increases result in activation of hypertrophic signaling pathways

In addition to its role in EC coupling and cardiac contraction, Ca^{2+} plays a well-recognized role in activation of hypertrophic signaling pathways [2]. To examine hypertrophic pathway stimulation we crossed STIM1 TG mice to mice containing a NFAT luciferase reporter transgene [26]. At 10–12 weeks of age we observed a significantly higher induction of

NFAT activity *in vivo* (Figure 7C), suggesting that STIM1-mediated Ca^{2+} entry can activate this pathological hypertrophic signaling pathway. Additionally, STIM1 TG hearts showed a subtle but significant enhancement in CaMKII activity (Figure 7D), likely also due to increased intracellular Ca^{2+} levels, although there was no change in total CaMKII δ protein (Figure 7E). This increased CaMKII activity also did not result in increased phosphorylation of the CaMKII or protein kinase A phosphorylation sites on RyR2 (Figure 7F), suggesting that the enhanced spark frequency observed in isolated STIM1 TG myocytes was not due to either of these post-translational modifications on RyR2. However, underlying the known enhancement in Ca^{2+} cycling in STIM1 TG myocytes, we did observe an increase in SERCA2 protein levels but no change in NCX1 compared with Wt control (Figure 7F).

4. Discussion

Pathological cardiac hypertrophy is characterized by re-expression of a fetal gene program consisting of *Nppa*, *Nppb*, *Acta1* and *Myh7* [30]. The Ca^{2+} sensor protein STIM1 is another factor that is highly-expressed in the developing heart that then switches to a low basal pattern of expression in the adult heart but that is upregulated in response to disease stimuli [13, 14]. Indeed, neonatal cardiac myocytes with shRNA-mediated knockdown of STIM1 [13, 15] or whole-body knockout of STIM1 [14] showed loss of Ca^{2+} entry after store depletion that was similar to the low level of SOCE observed in adult cardiac myocytes [13]. Our results presented here suggest that STIM1 re-expression in the adult heart during disease produces an additional Ca^{2+} augmentation that contributes to pathological cardiac hypertrophy, such as through calcineurin/NFAT signaling and possibly CaMKII, as well as contributes to a general state of Ca^{2+} overload that causes mitochondrial changes and whole organ pathology.

Other potential disease influences of STIM1 are suggested in the literature. For example, Collins et al. demonstrated that mice with cardiac-specific deletion of STIM1 develop ER stress [31] suggesting that STIM1 activity is required to preserve the normal ER/SR Ca^{2+} load required for the proper function of resident chaperones and for protein folding. In addition, cardiac STIM1 deleted mice displayed fragmented mitochondria due to increased mitochondrial fission, as well as a progressive dilated cardiomyopathy with decreased ejection fraction and fibrosis that resulted in death between 40 and 65 weeks of age [31]. Thus, while re-expression of STIM1 in the adult heart has clear pathologic consequences, it also appears to have homeostatic functionality in the adult heart at low baseline levels of expression. Indeed, recent studies have revealed that mitochondria associated membranes, which create close connections between the mitochondria and the ER/SR, can regulate transfer of Ca^{2+} from the ER to mitochondria, affecting electron transport chain function and likely overall metabolism [32].

Although SOCE mediates ER store refilling, STIM1 appears to have other mechanisms of action on intracellular Ca^{2+} handling in a cardiac myocyte that are partially independent of traditional SOCE through interaction with Orai1. Isolated STIM1 TG cardiac myocytes displayed spontaneous Ca^{2+} transients and a Ca^{2+} overload effect with increased spark frequencies and SERCA2 expression, but without an increase in total SR Ca^{2+} load or modification of RyR2, the latter of which is known to cause increases in spark frequency

[33]. These other actions of STIM1 could be due to its reported interaction with the LTCC C-terminus at the plasma membrane [18, 19]. Interestingly, we observed enhancement of LTCC activity at 2 months of age in STIM1 TG myocytes that could be related to greater CaMKII activity. However, we also observed that LTCC α_{1C} protein levels were reduced at the later 12 week time point. These alterations could have the effect of increasing myocyte Ca^{2+} load early on, contributing to increased diastolic Ca^{2+} and activation of pro-hypertrophic signaling pathways [34]. The augmented profile of Ca^{2+} fluxing and greater SR leak likely contributed to the sudden death observed in STIM1 TG mice, even though we failed to identify examples of arrhythmia under unstressed conditions (data not shown).

STIM1 may also contribute to a re-organization of Ca^{2+} handling proteins in the junctional SR space that could influence EC coupling and signaling. Upon activation, STIM1 multimerizes and moves from a diffuse distribution on the ER membrane to focal regions of interaction with the plasma membrane where they activate Ca^{2+} entry in approximation with Orai1 [16]. Recent reports have demonstrated that STIM1 can co-localize with LTCCs and Orai1 at ER/plasma membrane junctions [19]. Additionally, we have shown that STIM1 can partially co-localize with RyR2 and STIM1 has been demonstrated to associate with SERCA2 [20, 21] and the Na^+/K^+ ATPase [20]. This clustering of Ca^{2+} release (RyR2), Ca^{2+} entry (Orai1, LTCC) and Ca^{2+} uptake (SERCA2 and Na^+/K^+ ATPase with the $\text{Na}^+/\text{Ca}^{2+}$ exchanger) pathways could result in increased efficiency of Ca^{2+} cycling, perhaps explaining the faster decay time of the Ca^{2+} transient observed in STIM1 TG cardiac myocytes. It is also possible that STIM1 re-organization of Ca^{2+} entry and uptake machinery could alter the individual Ca^{2+} fluxes in a more subtle way. While increased SR Ca^{2+} load has been shown to increase spark frequency [33], it also typically results in an increase in spark amplitude [33]. STIM1 overexpression, on the other hand, results in reduced spark amplitude (Figure 5D). Small amplitude Ca^{2+} release has been previously associated with the activity of “rogue” RyR2 proteins arranged singly or in small clusters, as opposed to the prototypically organized Ca^{2+} release units that contain a large complement of RyR2 proteins arranged in close proximity to LTCCs [35]. It is intriguing to speculate that STIM1 overexpression might generate additional rogue RyR2 populations by either altering RyR2 channel organization or by otherwise altering its regional connectivity with LTCCs, perhaps by reducing the expression of the LTCC α_{1C} subunit, as we demonstrate in Figure 7B. We therefore speculate that overexpression of STIM1 results in widespread miscommunication between numerous Ca^{2+} handling pathways on the surface sarcolemma and junctional SR, including 1) increased diastolic Ca^{2+} load resulting from enhancement of SOCE, 2) increased expression of SERCA2 that aids in more rapid uptake of cytosolic Ca^{2+} into the SR and is balanced by 3) increased sensitivity of RyR2 that results in elevated spark frequency and SR Ca^{2+} leak, such that SR Ca^{2+} load is not increased, promoted by 4) dysregulation of LTCC activity that initially favors maximal activation of the channel but ultimately leads to reduced channel expression.

At a more fundamental level, it is also likely that overexpression of STIM1 results in elevated diastolic Ca^{2+} that activates pro-hypertrophic signaling to serve as the prime inducer of heart disease in this mouse model. Indeed, overexpression of TRPC3 or TRPC6 in the mouse heart, which also dramatically increases SOCE, similarly leads to cardiomyopathy and calcineurin-NFAT signaling [5, 7, 8]. Like STIM1, endogenous TRPC

activity is induced under cardiac stress stimulation where it directly contributes to disease. For example, inhibition of TRPC activity in the hearts of TG mice expressing dominant negative mutant TRPC proteins or in *Trpc1* KO mice, or mice treated with the specific TRPC3 inhibitor Pyr3 showed less hypertrophy or disease in response to pressure overload stimulation [6, 9, 10]. Collectively, these results underscore the potential importance of alternate Ca^{2+} influx currents that are induced in the adult diseased heart, which uniformly appears to be a maladaptive response. Hence, STIM1 may be a novel target to consider for pharmacological intervention in the treatment of heart disease.

Supplementary Material

Refer to Web version on PubMed Central for supplementary material.

Acknowledgments

Funding Sources

This work was supported by grants from the National Institutes of Health (to J.D. Molkenin and S.R. Houser). J.D. Molkenin was also supported by the Howard Hughes Medical Institute.

Abbreviations

AngII	angiotensin II
BDM	2,3-butanedione monoxime
CaMKII	Ca^{2+} /calmodulin-dependent protein kinase II
CMF	Ca^{2+} - and Mg^{2+} -free Ringer's solution
CPA	cyclopiazonic acid
EC	excitation-contraction
ER	endoplasmic reticulum
LTCC	L-type Ca^{2+} channel
NFAT	nuclear factor of activated T-cells
PE	phenylephrine
RyR	ryanodine receptor
SERCA2	sarcoplasmic/endoplasmic reticulum Ca^{2+} ATPase 2
SOCE	store-operated Ca^{2+} entry
SR	sarcoplasmic reticulum
STIM1	stromal interaction molecule 1
TAC	transverse aortic constriction
TG	transgenic
TRP	transient receptor potential

Wt wild-type

References

1. Katz AM. The "modern" view of heart failure: how did we get here? *Circulation Heart failure*. 2008; 1:63–71. [PubMed: 19808272]
2. Heineke J, Molkentin JD. Regulation of cardiac hypertrophy by intracellular signalling pathways. *Nature reviews Molecular cell biology*. 2006; 7:589–600. [PubMed: 16936699]
3. Chen X, Nakayama H, Zhang X, Ai X, Harris DM, Tang M, et al. Calcium influx through Cav1.2 is a proximal signal for pathological cardiomyocyte hypertrophy. *Journal of molecular and cellular cardiology*. 2011; 50:460–470. [PubMed: 21111744]
4. Makarewich CA, Correll RN, Gao H, Zhang H, Yang B, Berretta RM, et al. A caveolae-targeted L-type Ca(2)+ channel antagonist inhibits hypertrophic signaling without reducing cardiac contractility. *Circulation research*. 2012; 110:669–674. [PubMed: 22302787]
5. Bush EW, Hood DB, Papst PJ, Chapo JA, Minobe W, Bristow MR, et al. Canonical transient receptor potential channels promote cardiomyocyte hypertrophy through activation of calcineurin signaling. *The Journal of biological chemistry*. 2006; 281:33487–33496. [PubMed: 16950785]
6. Kiyonaka S, Kato K, Nishida M, Mio K, Numaga T, Sawaguchi Y, et al. Selective and direct inhibition of TRPC3 channels underlies biological activities of a pyrazole compound. *Proceedings of the National Academy of Sciences of the United States of America*. 2009; 106:5400–5405. [PubMed: 19289841]
7. Kuwahara K, Wang Y, McAnally J, Richardson JA, Bassel-Duby R, Hill JA, et al. TRPC6 fulfills a calcineurin signaling circuit during pathologic cardiac remodeling. *The Journal of clinical investigation*. 2006; 116:3114–3126. [PubMed: 17099778]
8. Nakayama H, Wilkin BJ, Bodi I, Molkentin JD. Calcineurin-dependent cardiomyopathy is activated by TRPC in the adult mouse heart. *FASEB journal : official publication of the Federation of American Societies for Experimental Biology*. 2006; 20:1660–1670. [PubMed: 16873889]
9. Seth M, Zhang ZS, Mao L, Graham V, Burch J, Stiber J, et al. TRPC1 channels are critical for hypertrophic signaling in the heart. *Circulation research*. 2009; 105:1023–1030. [PubMed: 19797170]
10. Wu X, Eder P, Chang B, Molkentin JD. TRPC channels are necessary mediators of pathologic cardiac hypertrophy. *Proceedings of the National Academy of Sciences of the United States of America*. 2010; 107:7000–7005. [PubMed: 20351294]
11. Collins HE, Zhu-Mauldin X, Marchase RB, Chatham JC. STIM1/Orai1-mediated SOCE: current perspectives and potential roles in cardiac function and pathology. *American journal of physiology Heart and circulatory physiology*. 2013; 305:H446–H458. [PubMed: 23792674]
12. Bers DM. Calcium cycling and signaling in cardiac myocytes. *Annual review of physiology*. 2008; 70:23–49.
13. Luo X, Hojaye B, Jiang N, Wang ZV, Tandan S, Rakalin A, et al. STIM1-dependent store-operated Ca(2)(+) entry is required for pathological cardiac hypertrophy. *Journal of molecular and cellular cardiology*. 2012; 52:136–147. [PubMed: 22108056]
14. Hulot JS, Fauconnier J, Ramanujam D, Chaanine A, Aubart F, Sassi Y, et al. Critical role for stromal interaction molecule 1 in cardiac hypertrophy. *Circulation*. 2011; 124:796–805. [PubMed: 21810664]
15. Voelkers M, Salz M, Herzog N, Frank D, Dolatabadi N, Frey N, et al. Orai1 and Stim1 regulate normal and hypertrophic growth in cardiomyocytes. *Journal of molecular and cellular cardiology*. 2010; 48:1329–1334. [PubMed: 20138887]
16. Soboloff J, Rothberg BS, Madesh M, Gill DL. STIM proteins: dynamic calcium signal transducers. *Nature reviews Molecular cell biology*. 2012; 13:549–565. [PubMed: 22914293]
17. Yuan JP, Zeng W, Huang GN, Worley PF, Muallem S. STIM1 heteromultimerizes TRPC channels to determine their function as store-operated channels. *Nature cell biology*. 2007; 9:636–645. [PubMed: 17486119]

18. Park CY, Shcheglovitov A, Dolmetsch R. The CRAC channel activator STIM1 binds and inhibits L-type voltage-gated calcium channels. *Science*. 2010; 330:101–105. [PubMed: 20929812]
19. Wang Y, Deng X, Mancarella S, Hendron E, Eguchi S, Soboloff J, et al. The calcium store sensor, STIM1, reciprocally controls Orai and CaV1.2 channels. *Science*. 2010; 330:105–109. [PubMed: 20929813]
20. Krapivinsky G, Krapivinsky L, Stotz SC, Manasian Y, Clapham DE. POST, partner of stromal interaction molecule 1 (STIM1), targets STIM1 to multiple transporters. *Proceedings of the National Academy of Sciences of the United States of America*. 2011; 108:19234–19239. [PubMed: 22084111]
21. Sampieri A, Zepeda A, Asanov A, Vaca L. Visualizing the store-operated channel complex assembly in real time: identification of SERCA2 as a new member. *Cell calcium*. 2009; 45:439–446. [PubMed: 19327826]
22. Goonasekera SA, Davis J, Kwong JQ, Accornero F, Wei-LaPierre L, Sargent MA, et al. Enhanced Ca(2)(+) influx from STIM1-Orai1 induces muscle pathology in mouse models of muscular dystrophy. *Human molecular genetics*. 2014; 23:3706–3715. [PubMed: 24556214]
23. Stiber J, Hawkins A, Zhang ZS, Wang S, Burch J, Graham V, et al. STIM1 signalling controls store-operated calcium entry required for development and contractile function in skeletal muscle. *Nature cell biology*. 2008; 10:688–697. [PubMed: 18488020]
24. DeHaven WI, Jones BF, Petranks JG, Smyth JT, Tomita T, Bird GS, et al. TRPC channels function independently of STIM1 and Orai1. *The Journal of physiology*. 2009; 587:2275–2298. [PubMed: 19332491]
25. Brennan KJ, Hardeman EC. Quantitative analysis of the human alpha-skeletal actin gene in transgenic mice. *The Journal of biological chemistry*. 1993; 268:719–725. [PubMed: 7678010]
26. Wilkins BJ, Dai YS, Bueno OF, Parsons SA, Xu J, Plank DM, et al. Calcineurin/NFAT coupling participates in pathological, but not physiological, cardiac hypertrophy. *Circulation research*. 2004; 94:110–118. [PubMed: 14656927]
27. Lynch JM, Maillet M, Vanhoutte D, Schloemer A, Sargent MA, Blair NS, et al. A thrombospondin-dependent pathway for a protective ER stress response. *Cell*. 2012; 149:1257–1268. [PubMed: 22682248]
28. Picht E, Zima AV, Blatter LA, Bers DM. SparkMaster: automated calcium spark analysis with ImageJ. *American journal of physiology Cell physiology*. 2007; 293:C1073–C1081. [PubMed: 17376815]
29. Nakayama H, Chen X, Baines CP, Klevitsky R, Zhang X, Zhang H, et al. Ca2+- and mitochondrial-dependent cardiomyocyte necrosis as a primary mediator of heart failure. *The Journal of clinical investigation*. 2007; 117:2431–2444. [PubMed: 17694179]
30. Dirks E, da Costa Martins PA, De Windt LJ. Regulation of fetal gene expression in heart failure. *Biochimica et biophysica acta*. 2013; 1832:2414–2424. [PubMed: 24036209]
31. Collins HE, He L, Zou L, Qu J, Zhou L, Litovsky SH, et al. Stromal interaction molecule 1 is essential for normal cardiac homeostasis through modulation of ER and mitochondrial function. *American journal of physiology Heart and circulatory physiology*. 2014; 306:H1231–H1239. [PubMed: 24585777]
32. de Brito OM, Scorrano L. An intimate liaison: spatial organization of the endoplasmic reticulum-mitochondria relationship. *The EMBO journal*. 2010; 29:2715–2723. [PubMed: 20717141]
33. Zima AV, Bovo E, Bers DM, Blatter LA. Ca(2)+ spark-dependent and -independent sarcoplasmic reticulum Ca(2)+ leak in normal and failing rabbit ventricular myocytes. *The Journal of physiology*. 2010; 588:4743–4757. [PubMed: 20962003]
34. Goonasekera SA, Hammer K, Auger-Messier M, Bodi I, Chen X, Zhang H, et al. Decreased cardiac L-type Ca(2)(+) channel activity induces hypertrophy and heart failure in mice. *The Journal of clinical investigation*. 2012; 122:280–290. [PubMed: 22133878]
35. Brochet DX, Xie W, Yang D, Cheng H, Lederer WJ. Quark calcium release in the heart. *Circulation research*. 2011; 108:210–218. [PubMed: 21148431]

Highlights

- STIM1 transgenic mice showed increased Ca^{2+} entry following store depletion.
- STIM1 transgenic mice develop cardiac hypertrophy and sudden death.
- Mitochondrial structure is compromised in STIM1 transgenic mouse hearts.
- STIM1 transgenic mice are predisposed to increased disease following insult.
- Myocytes isolated from STIM1 transgenic mice have elevated spark frequency.

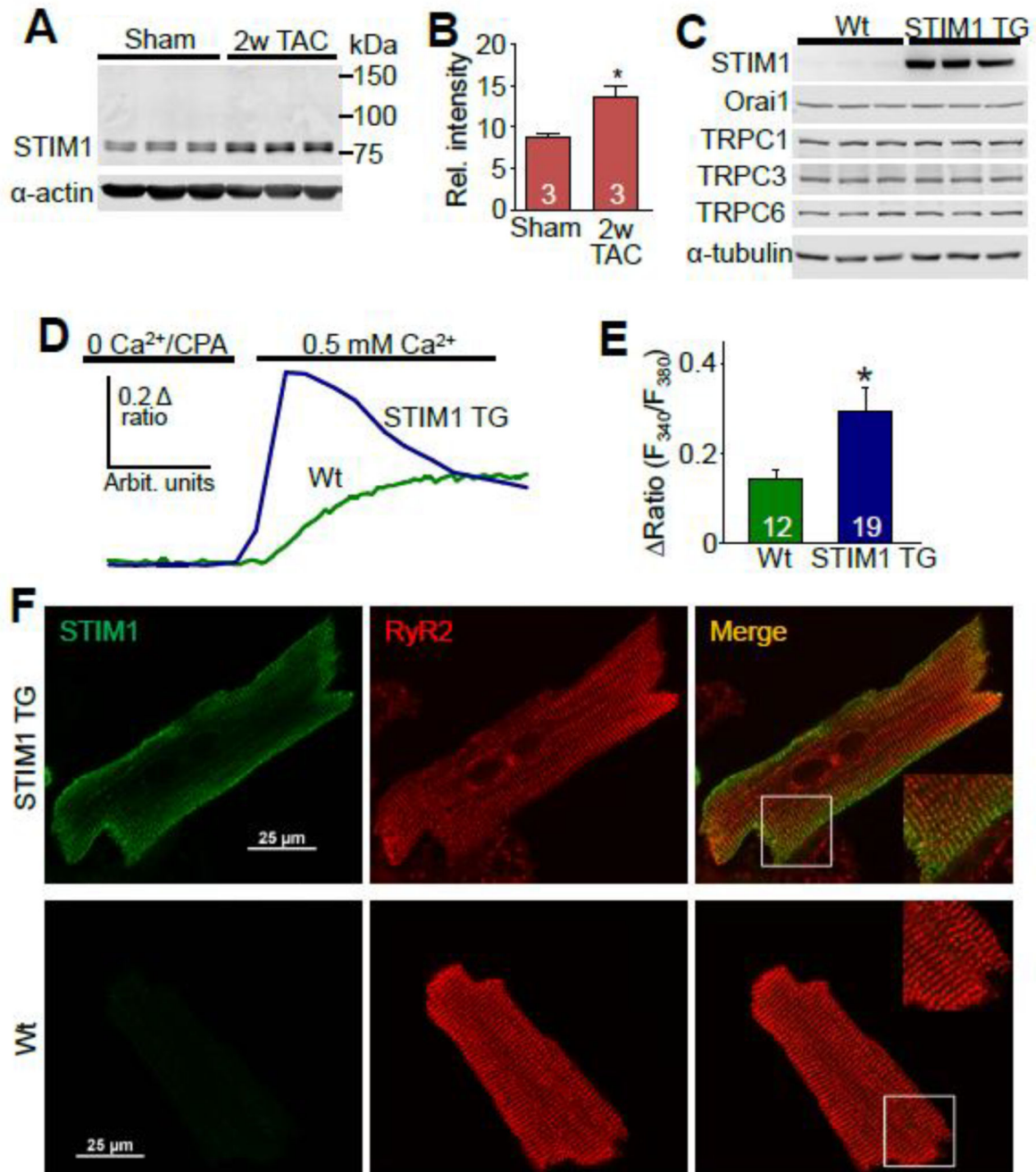


Figure 1. STIM1 overexpression results in increased Ca^{2+} entry after store depletion

(A) Immunoblots for STIM1 and α -sarcomeric actin protein from heart homogenates derived from wild-type (Wt) mice subjected to a sham procedure or pressure overload by TAC surgery for 2 weeks and (B) quantification of protein expression. (C) Immunoblots for STIM1, Orai1, TRPC1, TRPC3, TRPC6, and α -tubulin from Wt and STIM1 TG heart homogenates. (D) Ca^{2+} traces for store repletion in adult cardiac myocytes isolated from Wt or STIM1 TG mice, quantified in (E) with number of myocytes indicated in the graph.

* $P < 0.05$ vs Wt control. CPA (cyclopiazonic acid) is a SERCA inhibitor. (F) Confocal

immunofluorescence demonstrating partial co-localization at the cell periphery of STIM1 (green) and RyR2 (red) in myocytes isolated from adult Wt or STIM1 TG hearts.

Author Manuscript

Author Manuscript

Author Manuscript

Author Manuscript

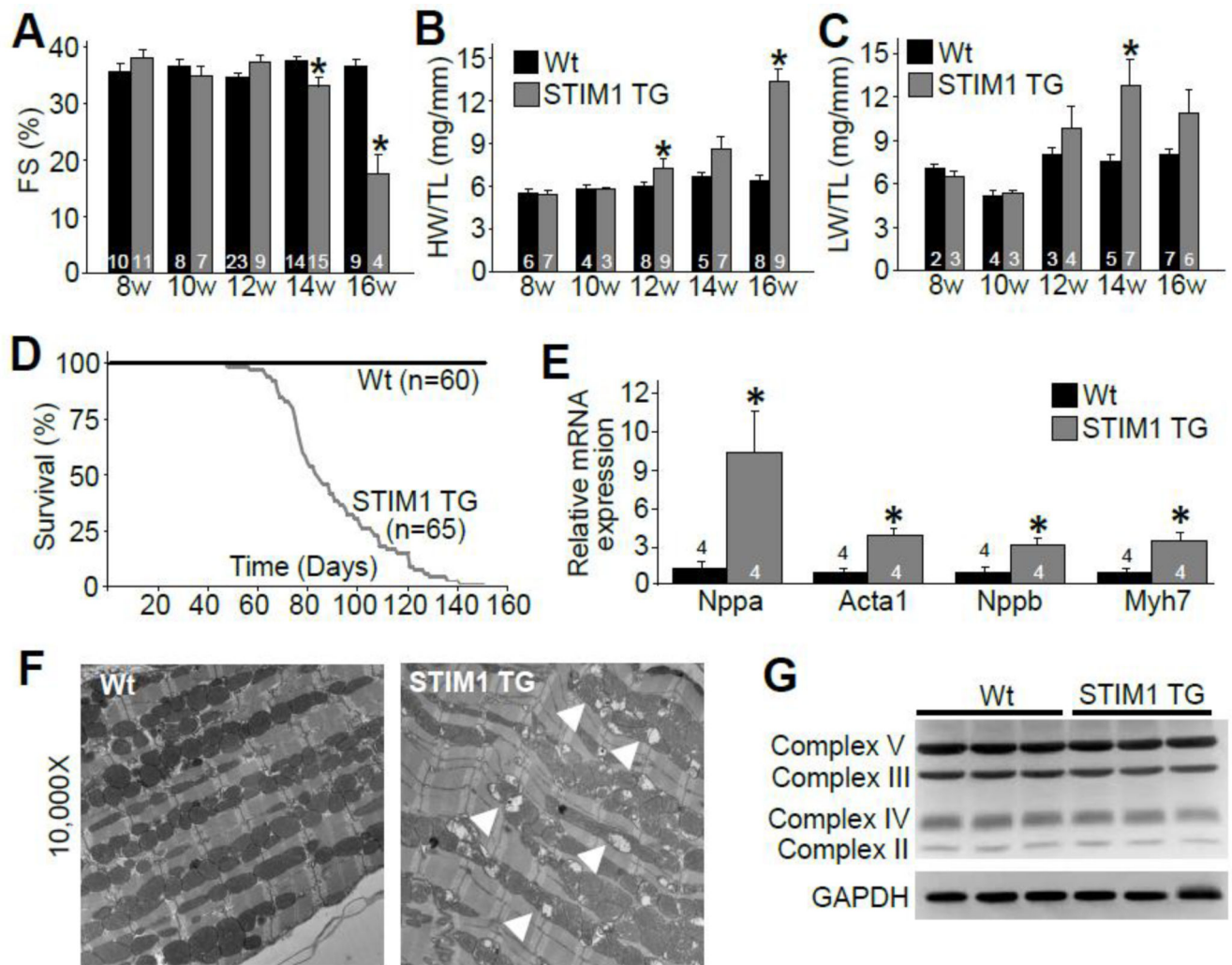


Figure 2. STIM1 overexpression results in cardiac disease

(A) Fractional shortening (FS) measured by echocardiography, (B) hypertrophy measured by heart weight to tibia length ratio (HW/TL), and (C) pulmonary edema measured by lung weight to tibia length ratio (LW/TL) in Wt and STIM1 TG mice at 8–16 weeks of age. (D) Kaplan-Meier survival curve is shown for Wt and STIM1 TG mice from birth to 22 weeks of age. (E) Relative mRNA expression for atrial natriuretic factor (*Nppa*), skeletal muscle α -actin (*Acta1*), brain natriuretic peptide (*Nppb*), and β -myosin heavy chain (*Myh7*) measured via quantitative polymerase chain reaction from Wt and STIM1 TG hearts at 12 weeks of age. (F) Transmission electron micrograph of sections from 10–12 week-old Wt and STIM1 TG hearts at 10,000 \times magnification. Arrows indicate swollen mitochondria with loosely-packed cristae. (G) Immunoblots for mitochondrial electron transport chain proteins and GAPDH from Wt and STIM1 TG heart homogenates. For each experiment, number of mice analyzed is given within the bars of the graphs. * $P < 0.05$ vs Wt control.

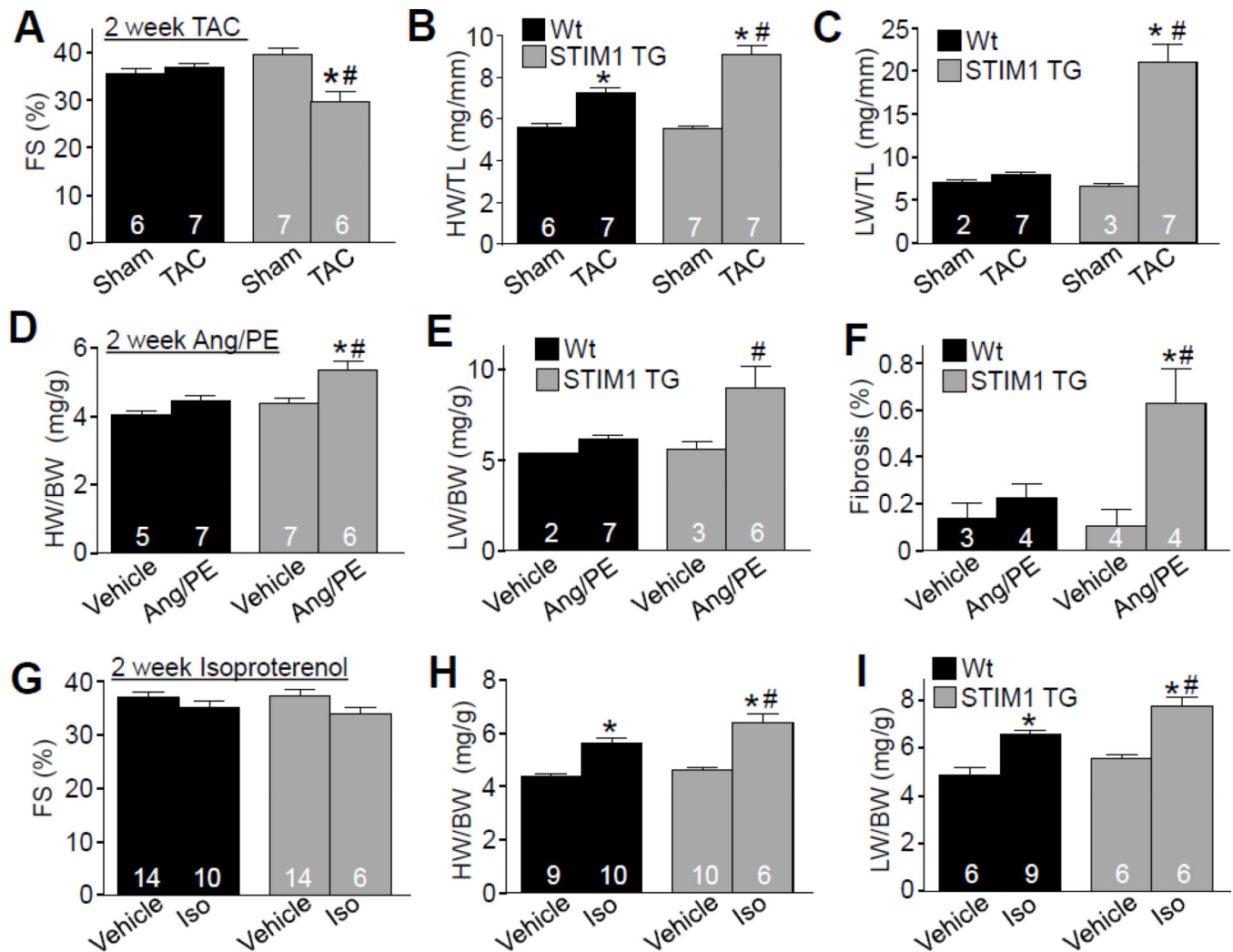


Figure 3. STIM1 transgenic mice are predisposed to increased cardiac disease after insult
 (A) Fractional shortening (FS) measured by echocardiography and measures of (B) hypertrophy by heart weight to tibia length ratio (HW/TL) and (C) pulmonary edema by lung weight to tibia length ratio (LW/TL) from Wt or STIM1 transgenic mice after 2 weeks of TAC or sham surgery. (D) Hypertrophy measured by heart weight to body weight ratio (HW/BW), (E) pulmonary edema by LW/BW, and (F) fibrosis measured after Masson's trichrome staining and Metamorph quantitation from Wt or STIM1 TG mice after 2 weeks of AngII/PE infusion via implanted osmotic minipumps. (G) FS measured by echocardiography and measures of (H) hypertrophy by HW/BW and (I) pulmonary edema by LW/BW from Wt or STIM1 TG mice after 2 weeks of isoproterenol infusion via implanted osmotic minipumps. For each experiment, number of mice analyzed is given within the bars in the graphs. *P<0.05 vs sham treatment of the same genotype; #P<0.05 vs WT TAC/agonist.

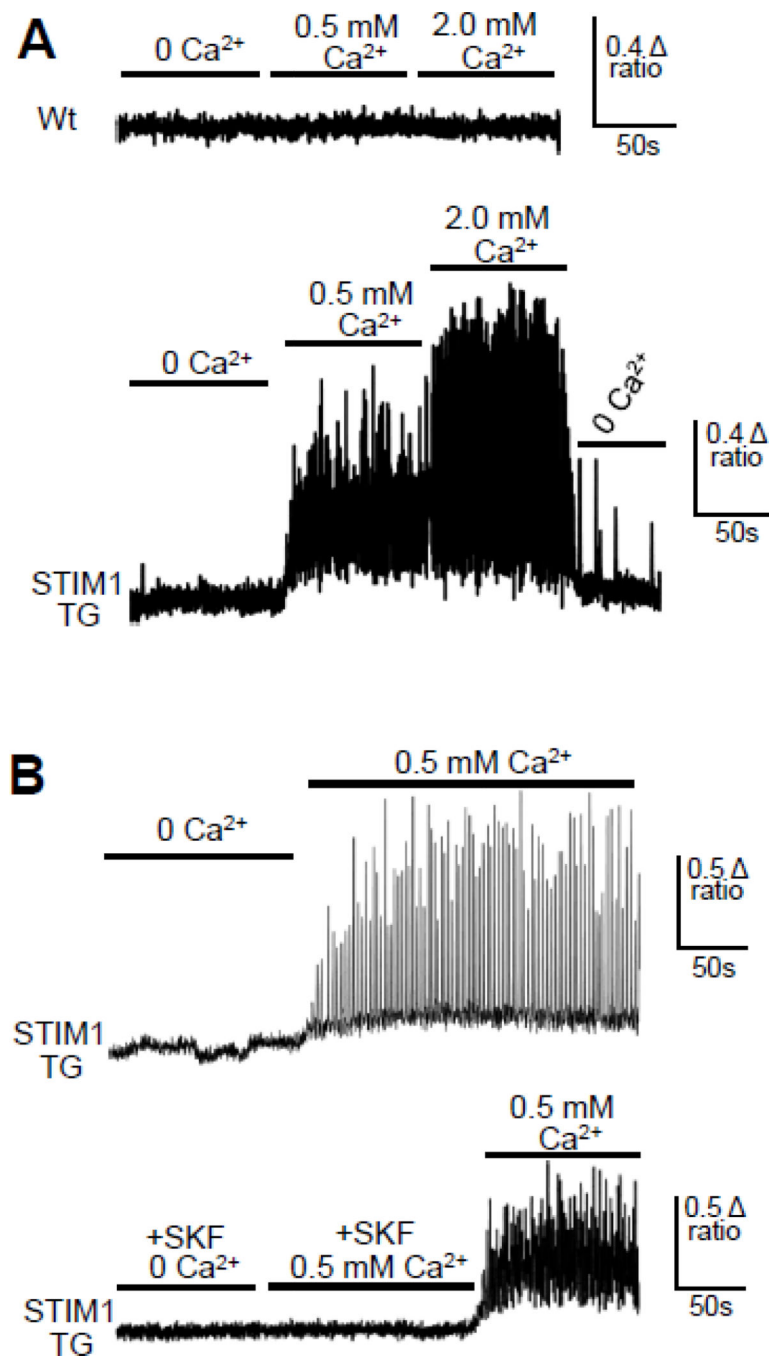


Figure 4. Cardiac myocytes isolated from STIM1 TG hearts show spontaneous Ca^{2+} transients (A) Ca^{2+} traces from unstimulated Fura-2 loaded isolated cardiac myocytes from Wt or STIM1 TG hearts in bath solution containing various concentrations of Ca^{2+} . (B) Ca^{2+} traces from unstimulated Fura-2 loaded isolated cardiac myocytes from STIM1 TG hearts in bath solution containing various concentrations of Ca^{2+} in the presence or absence of SKF-96365.

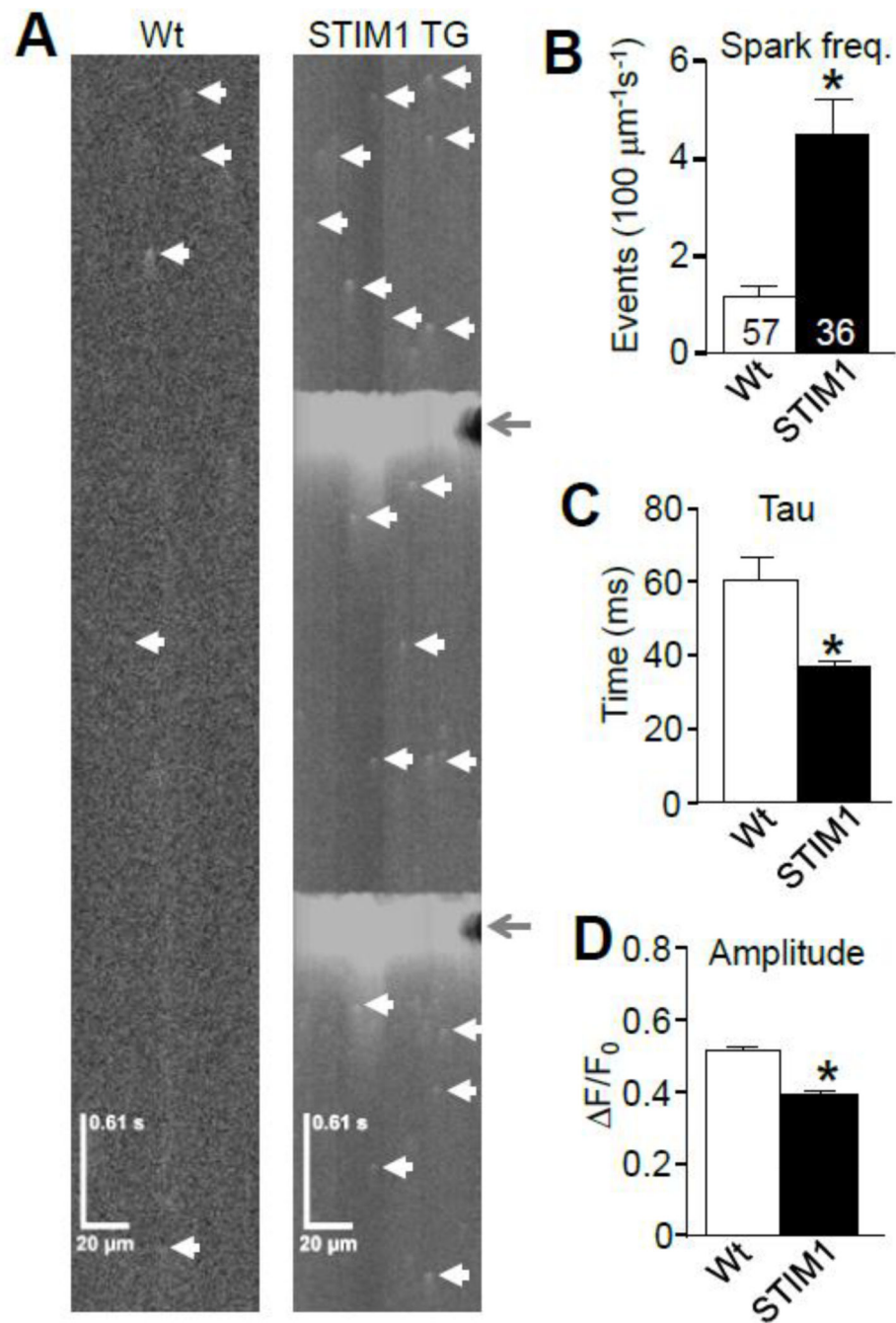


Figure 5. Increased Ca^{2+} spark frequency in cardiac myocytes isolated from STIM1 TG hearts (A) Representative confocal line scan images, as well as (B) spark frequency, (C) spark decay time constant (Tau), (D) and spark amplitude measured from cardiac myocytes isolated from Wt and STIM1 TG hearts at 11 weeks of age. Sparks are indicated by white arrowheads. Ca^{2+} waves observed in the STIM1 TG myocytes are indicated by the gray arrows. For Figures 5B–D, number of cardiac myocytes analyzed is given within the bars of the graphs in Figure 5B. Myocytes were isolated from at least three animals for each condition. * $P < 0.05$ vs Wt control.

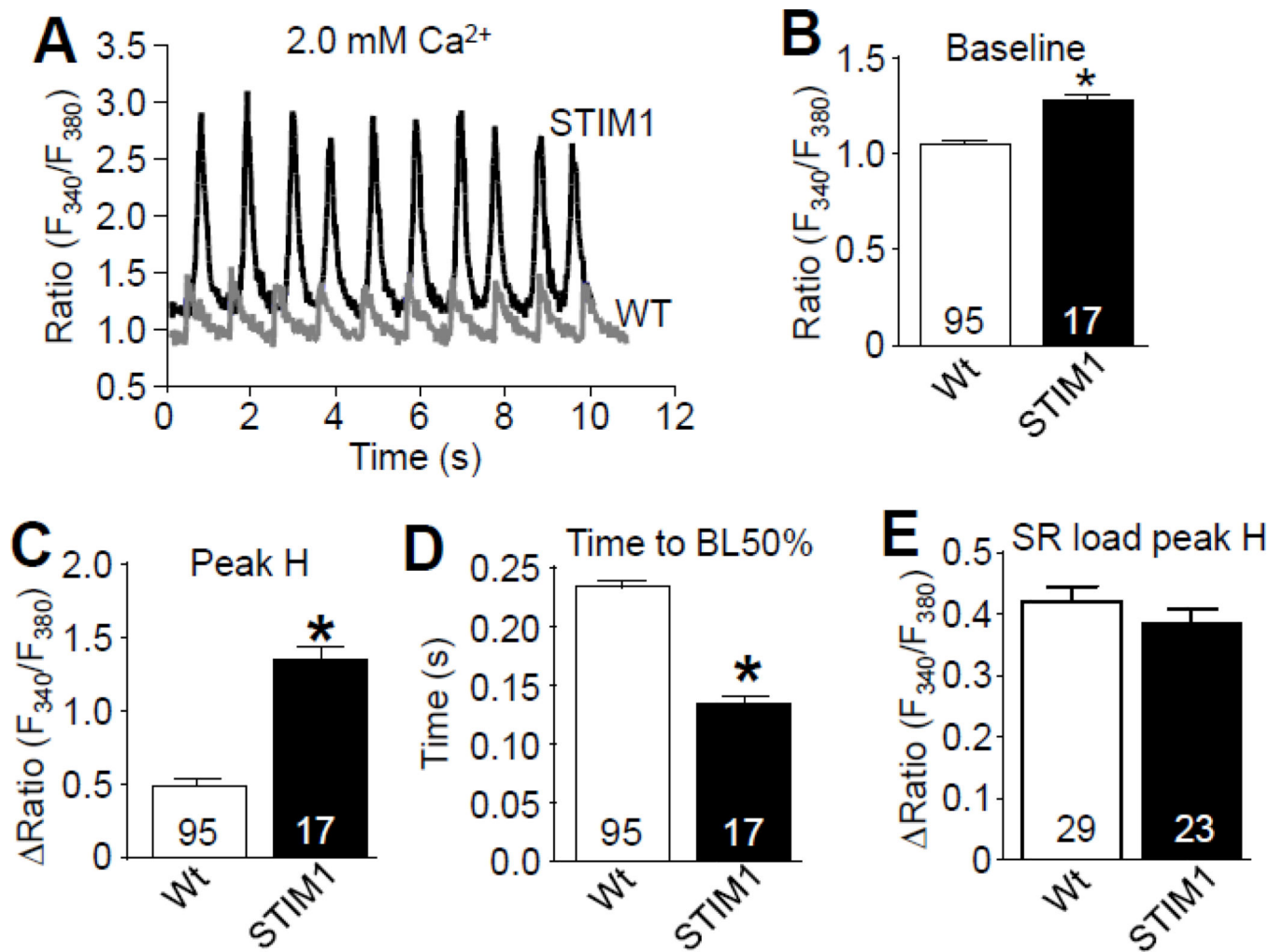


Figure 6. Ca^{2+} handling is altered in cardiac myocytes isolated from STIM1 TG hearts
 (A) Representative Ca^{2+} traces, as well as (B) diastolic Ca^{2+} , (C) mean maximal amplitude of electrically-evoked Ca^{2+} transients and (D) Ca^{2+} decay time measured from cardiac myocytes in 2 mM Ca^{2+} isolated from Wt and STIM1 TG hearts at 11 weeks of age. (E) SR Ca^{2+} load measured from 8–9 week-old Wt and STIM1 TG myocytes at 0.5 mM Ca^{2+} via caffeine-induced Ca^{2+} release. For Figures 6B-E, number of cardiac myocytes analyzed is given within the bars of the graphs. Myocytes were isolated from at least 3 animals for each condition. * $P < 0.05$ vs Wt control.

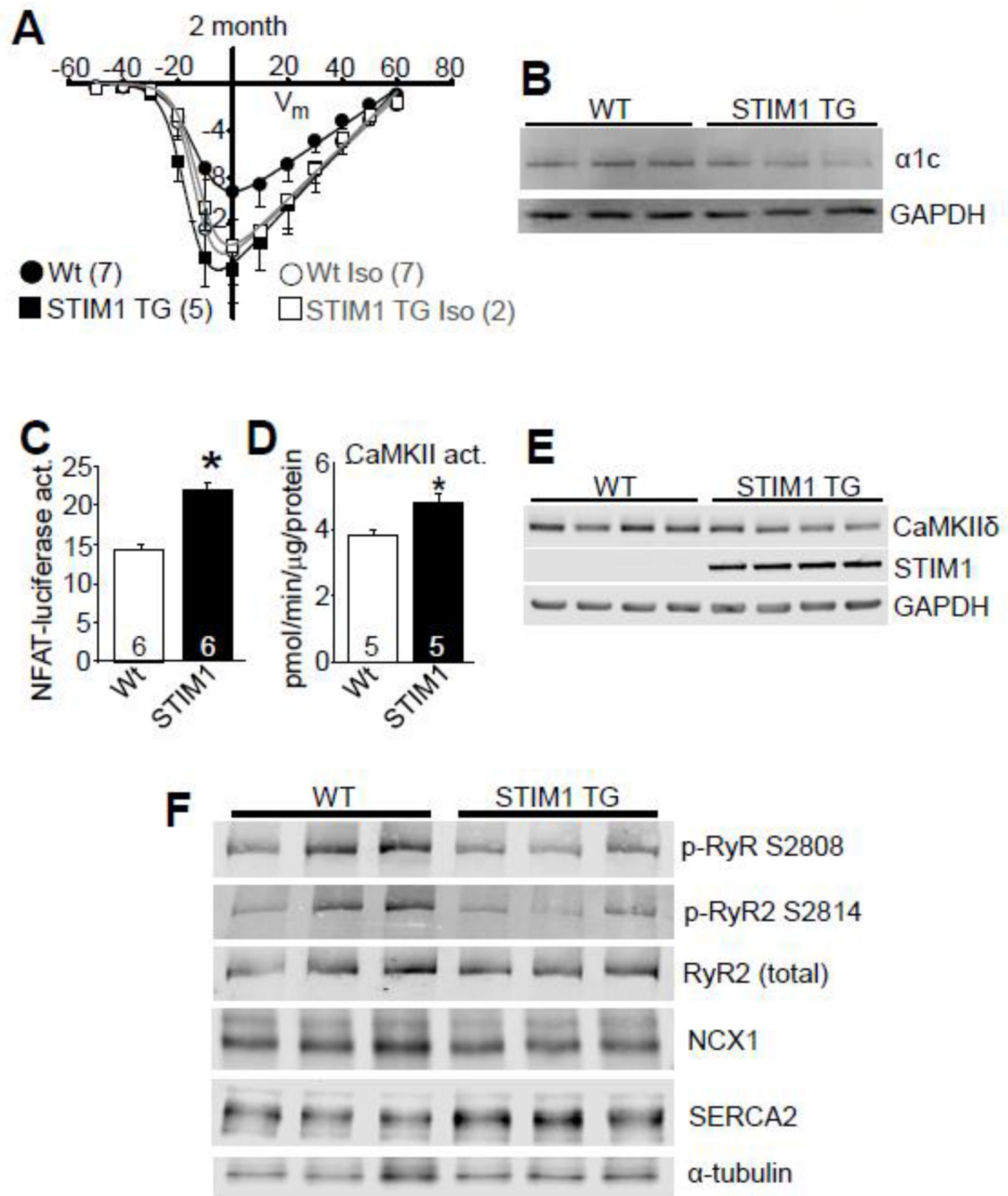


Figure 7. STIM1 TG mice show remodeling of Ca^{2+} handling and signaling pathways
 (A) Current-voltage relationships measured in whole-cell patch clamp experiments in myocytes isolated from Wt or STIM1 TG animals at 2 months of age, in the presence or absence of the β -adrenergic agonist isoproterenol. (B) Immunoblots for α_{1C} of the LTCC and GAPDH control from Wt or STIM1 TG hearts at 12 weeks of age. (C) NFAT luciferase activity measured in cardiac lysates from Wt and STIM1 TG hearts at 10–12 weeks of age that also contained the NFAT-luciferase reporter transgene. (D) Ca^{2+} -dependent CaMKII activity measured from Wt and STIM1 TG heart homogenates. (E) Immunoblots for

CaMKII δ , STIM1 and GAPDH protein from Wt and STIM1 TG heart homogenates. (F) Immunoblots of RyR2 phosphorylation at the 2 indicated sites and total RyR2, NCX1, and SERCA2 protein levels with α -tubulin control from Wt and STIM1 TG heart homogenates. For Figure 7A, number of cardiac myocytes analyzed is given within the graph. For Figure 7C-D, number of mice analyzed is given within the bars of the graphs. *P<0.05 vs Wt control.

Author Manuscript

Author Manuscript

Author Manuscript

Author Manuscript